Turk J Elec Engin, VOL.16, NO.1 2008, © TÜBİTAK

From Engineering Electromagnetics to Electromagnetic Engineering: Using Computational Electromagnetics for Synthesis Problems

Anton G. TIJHUIS, Martijn C. van BEURDEN, Bastiaan P. de HON, Hubregt J. VISSER
Faculty of Electrical Engineering, Eindhoven University of Technology
P.O. Box 513, 5600 MB Eindhoven, the Netherlands
e-mail: a.g.tijhuis@tue.nl

Abstract

In this paper, a two-stage approach is proposed for using computational electromagnetics in antenna engineering. First, stochastic optimization techniques are used in combination with approximate models. Second, line-search techniques are combined with full-wave modeling. For the first stage, we show an illustrative example. The second stage is considered in detail; both the acceleration of the underlying field computations and the implementation of the optimization are discussed.

1. Introduction

The increasing complexity and high speed of devices in electrical engineering makes the wave character of the underlying physical phenomena increasingly more important. In telecommunications, radar as well as astronomy, there is a common need for integrated antennas. In addition, such antennas must be used for multiple functions. In RF structures, particularly the response of the interconnects requires the evaluation of electromagnetic fields in three dimensions. In EMC problems, the local behavior of a wiring network may affect the entire system. In all of these examples, the proximity of parts of the structure is such that probing the field causes a significant disturbance. Further, only a limited number of "observables" is extracted from the three-dimensional field.

This raises the question how computational electromagnetics can be used to analyze or even design such structures. In all cases, the complexity and the size of the device prevent a direct application of brute-force computational techniques. On the other hand, parts of such a geometry can be analyzed with state-of-the-art algorithms. In this paper, we elaborate on this situation and describe elements of an approach towards handling the desired complexity. At this time, we cannot show the application of the complete approach to a single synthesis problem. However, for each step, either references or an illustrative example will be given to demonstrate the feasibility of our ideas.

The paper is organized as follows. In Section 2, we describe the general approach, which consist of two stages. For the first stage, where approximate or reduced models are combined with stochastic optimization, a representative example is given in Section 3. Sections 4 and 5 then discuss in more detail the second stage,

where full-wave modeling is combined with a line-search based optimization strategy. In Section 6, finally, we arrive at some conclusions.

2. Towards Electromagnetic Engineering

In the industrial design of a microwave or antenna system, typically two steps are followed. In the first stage, an extracted or equivalent model is optimized using one of the many available computational optimization strategies. In the second stage, a prototype of the resulting first-order model is realized in hardware, and fine-tuned with the aid of experimental techniques. In both stages, human intelligence is needed to steer the process, in particular with respect to the choice of the design criteria and the choice of the direction in which the improvement or "update" is sought. This intelligence is usually obtained from a few experienced engineers, which makes the design process vulnerable and expensive. This raises the question whether computational techniques can be used to augment or even replace this process.

Engineering Electromagnetics has reached the state where commercial software seems capable of replacing some or all of the prototyping in the second stage. However, a single electromagnetic-field computation for a complicated three-dimensional configuration that is representative of an actual microwave or antenna device may still take hours or days. Thus, like in prototyping, only a few geometries are analyzed before the design is finalized. Stochastic techniques are capable of searching an optimum in a large parameter space with multiple local optima. However, they could have to consider many thousands of "candidates" for each of which the electromagnetic behavior needs to be analyzed. Using state-of-the-art computational electromagnetics for this purpose does not seem realistic for the foreseeable future.

This indicates that Electromagnetic Engineering, which aims at using computational electromagnetics in the synthesis problem, should follow a two-step strategy similar to the current industrial process. In the first stage, stochastic optimization is applied to approximate models that allow a fast evaluation of the cost or fitness function. Equivalent circuits or extracted parameters as they are widely used in engineering practice may be suitable for this purpose. An alternative approach is reduced-order modeling [1,2], which is capable of reducing the size of a linear system of equations for an unknown field quantity to a much smaller system in which the behavior of relevant physical parameters is preserved.

In the second stage, we assume that a suitable initial estimate is available, either from the first stage or from engineering experience. Thus, local optima are avoided, and deterministic algorithms based on a local linearization may be employed for the optimization. Even this requires the evaluation of the electromagnetic behavior of tens of candidates, so that the computation time must be reduced "from hours to minutes" for this procedure to be realistic.

Detection and synthesis problems have a lot in common. In both cases, the field in a configuration must be matched to specifications by a combination of modeling and optimization. For the simulations, this means that we must evaluate the field in a known geometry with a varying physical or line-search parameter. The difference lies in the formulation of the cost function for the optimization. For a detection problem, this involves a weighted least-squares summation over the deviation between the observed and the simulated field. In addition, the existence of an object is obvious, while its identity, shape and/or constitution must be determined uniquely. In a synthesis problem, the existence of a solution for a given specification is not *a priori* clear, while its uniqueness is less important. In the synthesis problem, therefore, the proper formulation of the cost function is a major challenge.

Last but not least, a device should be fault-tolerant. First, the design must account for variations due to the manufacturing. As an example, we mention the "profile dip" in optical fibers, which may show up

in the fabrication of the preform from which the fiber is drawn [3]. The influence of such variations can be determined from the sensitivities that are used to determine the search directions in line-search optimization. Second, the device may have to function in a varying environment. Here, the antenna in a mobile telephone may be a good example. The effect of such an environment can only be analyzed with the aid of a stochastic analysis.

3. Stochastic Optimization

In this section, we discuss the first stage as described in Section 2. Techniques like simulated annealing [4], genetic algorithms [5, 6] and particle-swarm optimization [7, 8] have been discussed extensively in the recent literature. Here, we limit ourselves to an example of using such a technique in combination with an analytic model to resolve a practical design problem.

We consider the case of an intravascular antenna, to be used as a tracking or imaging device in MRI. The antenna consists of a discrete number of coils wound around a cylindrical antenna body. In the quasi-static approximation, the magnetic field due to a straight line segment carrying a constant current is given by an analytic expression based on the Biot-Savart law. The superposition principle is then used to determine the field due to the complete antenna, approximating one circumference by twelve such segments. The availability of an analytic model makes it possible to synthesize antenna designs automatically. We have opted for a genetic algorithm, because of its "natural" appeal and ease in software implementation. The maximum number of coils is three, the height of every coil is allowed to vary between 0.1 mm and 4 mm, the gap between two adjacent coils may vary between 0.1 mm and 3 mm, the number of turns per coil may vary between one and fifteen, and every coil may be wound clockwise and counterclockwise. The radius of the antenna is 1 mm. We have generated designs for tracking and imaging.

First, we consider an antenna for tracking purposes. As fitness parameter, we choose the minimum value of the sensitivity parameter, sampled over the z-axis of the antenna, between 3 mm and 6 mm from the base of the antenna. The sensitivity parameter expresses the susceptibility of the intravascular antenna to the magnetic field of the MRI device as a function of position. The sensitivity parameter is defined as $S = \frac{1}{I}\sqrt{B_x^2 + B_y^2}$ (TA^{-1}), where $B_\alpha = \mu H_\alpha$, $\alpha = x, y$ and where I is the current flowing through the antenna.

The optimization is a maximization process, so by selecting the fitness parameter in this manner we demand a high sensitivity on axis in the given interval. The optimization process generates (within a few minutes) a design consisting of three coils. The first coil starts at 2.64 mm from the antenna base. The heights of the coils, counting from bottom to top are 3.76 mm, 3.75 mm and 3.13 mm, the number of turns are 13, 5 and 1. The gaps between the coils are 2.91 mm and 2.64 mm. The first and third coils are wound counterclockwise, the second coil is wound clockwise. Sensitivity profiles in the xz-, yz- and xy-planes are shown in Figure 1. It is observed that indeed between 3 mm and 6 mm from the antenna base an increased sensitivity is achieved on the central axis of the antenna body. However, the sensitivity is still below the sensitivity obtained at the surface of the antenna body. So, the optimization procedure works, but more care should be taken in formulating the fitness parameter. Alternatively, one could aim at an increased sensitivity on the antenna body surface.

As a second example, we generate an antenna for imaging purposes. As a fitness parameter, we use the minimum value for the sensitivity parameter, sampled over the outer surface of a cylinder with a radius of 2.5 mm encapsulating the antenna, between 3 mm and 6 mm in height. The optimization process generates

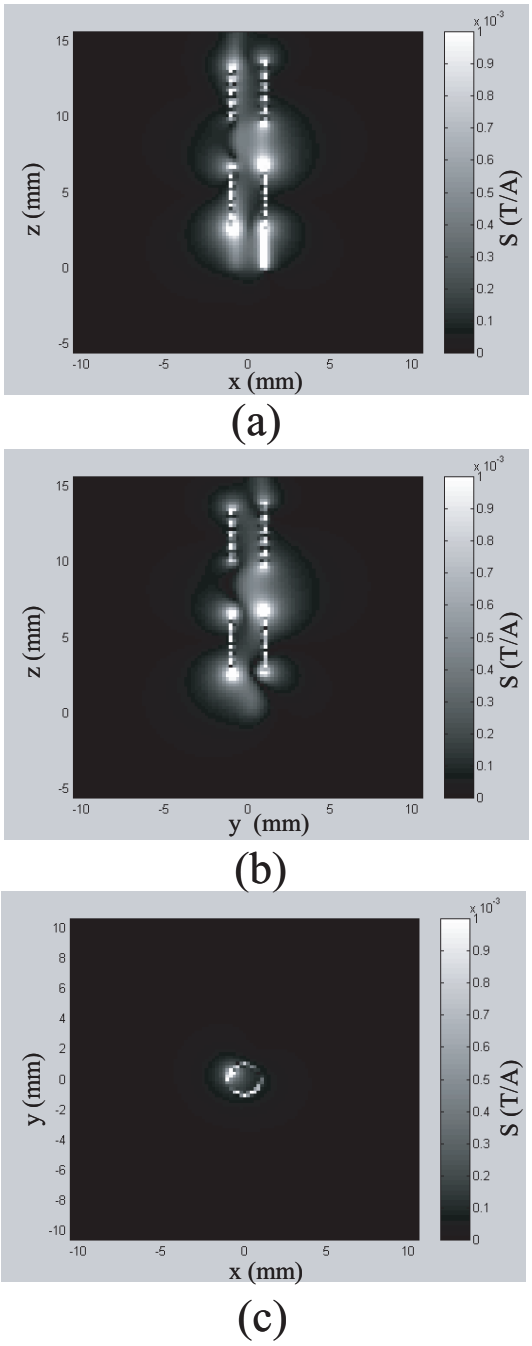

Figure 1. Sensitivity patterns in xz-, yz-, and xy-planes for multiple coil antenna optimized for tracking. (a) xz-plane, $y = 0.05$ mm; (b) yz-plane, $x = 0.05$ mm; (c) xy-plane, $z = 4.5$ mm.

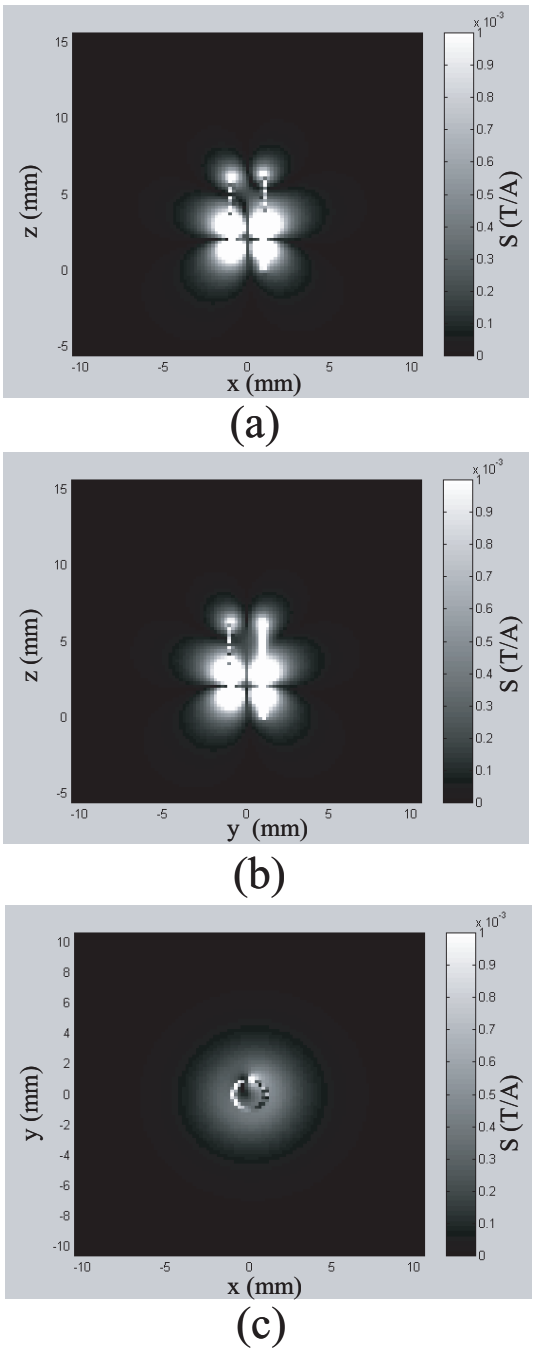

Figure 2. Sensitivity patterns in xz-, yz-, and xy-planes for multiple coil antenna optimized for imaging. (a) xz-plane, $y = 0.05$ mm; (b) yz-plane, $x = 0.05$ mm; (c) xy-plane, $z = 4.5$ mm.

(within a few minutes) a design consisting of three coils. The first coil starts at 1.73 mm from the antenna base. The height of the coils, counting from bottom to top are 0.41 mm, 0.12 mm and 3.20 mm. The gaps between the coils are 0.28 mm and 0.19 mm. All coils are wound counterclockwise. Sensitivity profiles in the xz-, yz- and xy-planes are shown in Figure 2. This figure shows that we have made a better choice for the fitness parameter this time. A strong and rotationally invariant sensitivity is visible in the radial and axial ranges specified. The values of heights and gap widths, however, suggest that an accurate and reproducible construction method is needed to manufacture the antennas.

The procedure outlined above can be improved upon in two ways. First, starting from the designs obtained by the genetic algorithm, one could employ a line-search based optimization to reach a better local optimum of the analytic fitness function. Second, the analytic model could be replaced by a standard thin-wire code like NEC to obtain more accurate values for the magnetic field. The high sensitivity of the fitness function with respect to the values of the design parameters indicates that one or both elements of this second stage, as described in Section 2, may be needed to obtain a satisfactory design.

4. Forward Modeling

In the remainder of this paper, we concentrate on this second stage, where an initial estimate is available. In that part of the design process, full-wave modeling must be combined with line-search optimization, which amounts to successive sweeps with respect to a line-search parameter. Two concepts have been developed by our team to reduce the duration of a single field computation "from hours to minutes," so that it may be repeated tens of times in the optimization.

4.1. Marching on in Anything

The first concept concerns the solution of field problems for a varying physical parameter [9]. The parameter may be frequency, angle of incidence, object dimension, or a combination of physical quantities combined in a line-search parameter in an optimization step. After discretization, the field problem assumes the form of a linear system of equations

$$L(p)\,u(p) = f(p), \tag{1}$$

where $u(p)$ is a discretized field and $f(p)$ corresponds to the excitation. We are interested in the situation where this problem must be solved for a large number of sampled values of the parameter p, e.g., $p_m = p_0 + m\Delta p$, with $m = 0, 1, \ldots, M$. To this end, we minimize the squared error

$$\mathrm{ERR}^{(n)} = ||r^{(n)}||^2 =< r^{(n)} \mid r^{(n)} >, \tag{2}$$

with $r^{(n)} = Lu^{(n)} - f$ with the aid of a standard conjugate gradient method. This procedure is accelerated significantly when the initial estimate for $p = p_m$ is generated from a few previous "final" results, according to the relation

$$u^{(0)}(p_m) = \sum_{k=1}^{K} \gamma_k\, u(p_{m-k}), \tag{3}$$

where the $\{\gamma_k \mid k = 1, \ldots, K\}$ are found by minimizing the squared error (2). The value of the coefficients $\{\gamma_k\}$ can be found from the system of linear equations

$$\sum_{k=1}^{K} < L(p_m)u(p_{m-\ell}) \mid L(p_m)u(p_{m-k}) > \gamma_k$$
$$=< L(p_m)u(p_{m-\ell}) \mid f(p_m) >, \tag{4}$$

with $\ell = 1, \ldots, K$. The procedure has been demonstrated for boundary and domain integral equations in two and three dimensions [9]. Typically $K = 2$ or $K = 3$, i.e., storing two or three previous final results suffices, and the acceleration rate varies between 10 and 50.

For "finite" (difference or element) methods, the solution of the discretized equation (1) as such is less efficient because of the poor convergence of the conjugate gradient method. This can be explained from the structure of the adjoint operator which is employed to generate the update directions. This operator now links a few local field values, so that the update remains local as well. This problem can be remedied by applying a preconditioner based on a spectral decomposition of the discretized field. This opens up the possibility to combine the resulting preconditioned scheme with the extrapolation procedure outlined above.

4.2. Diakoptics

The second idea is to separate a large, complicated configuration into smaller subdomains. The electromagnetic field in these subdomains is then computed locally, for a simpler environment. Subsequently, the thus obtained field distributions are used as basis functions in a global version of the method of moments. This may be regarded as an application of Gabriel Kron's concept of diakoptics in electromagnetic field analysis.

This approach is increasingly used in modeling large, finite antenna arrays consisting of metallic patches. The currents on these patches are determined for an isolated patch and/or for a patch in an infinite array. In the synthetic functions (SFX, [10]) and characteristic basis function (CBF, [11]) approaches, this is achieved by moving an elementary source in the vicinity of the patch, and using singular-value decomposition to extract independent distributions. In the eigenfunction approach [12], the eigencurrents of the integral operator for the isolated patch are used as basis functions. Thus, the choice of the varying excitation and the subsequent SVD are avoided. These methods have already been applied successfully to structures consisting of electrically isolated domains, while overlapping basis functions for electrically connected domains are emerging [10]. In all cases, the metallic surface on which the induced electric surface currents are computed is subdivided.

An alternative is to subdivide the entire three-dimensional space. Typically, we consider an observation domain and an environment. The environment is supposed to be fixed, while the constitution of the observation domain is varied and optimized. Again, different possibilities exist to realize this concept. For closed or fully periodic structures a decomposition into modes has led to the multimode equivalent network approach [13]. In recent years, this method has been extended from waveguiding structures to periodic antenna arrays. The introduction of the concept of accessible modes, which restricts the analysis to those modes that are observed in a homogeneous region between sharp interfaces, has led to a significant increase in the computational efficiency.

In LEGO (Linear Embedding via Green's Operators, [14, 15]), the equivalence principle is used to model the interaction between different subdomains. The advantage is that this method is applicable to boundaries of arbitrary shape. To explain the basic principle, let us consider the two-dimensional multiple-

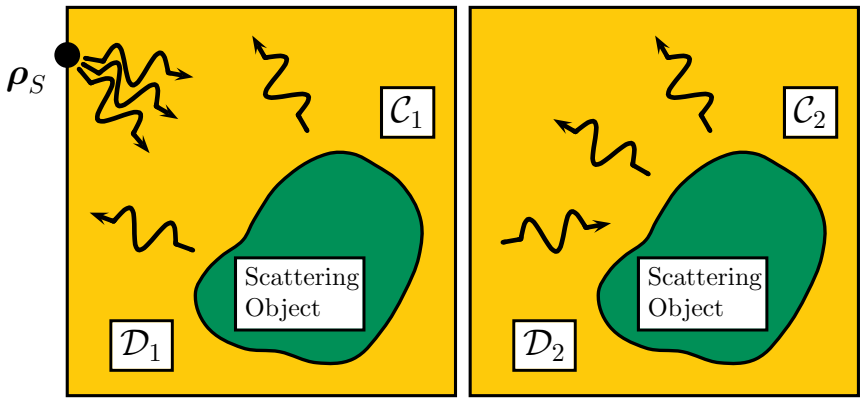

Figure 3. Excitation of two scattering objects in domains $\mathcal{D}_1$ and $\mathcal{D}_2$.

scattering problem shown in Figure 3. An electrically polarized line source is exciting two identical scattering objects, and the aim is to evaluate the electromagnetic field in an efficient manner. In LEGO, we proceed as follows.

- First, the scattering problem is solved for an isolated object in domain $\mathcal{D}$ with a homogeneous environment in the complementary domain $\bar{\mathcal{D}}$, excited by a line source on the boundary $\mathcal{C}$. Using the equivalence principle, the resulting scattered field in $\bar{\mathcal{D}}$ is then translated into one originating from an equivalent current on $\mathcal{C}$, e.g., by solving an EFIE. This equivalent current distribution is used to define a "scattering operator" for a single object.

- Second, we place a single object in $\mathcal{D}_1$, and choose the location of a line source on $\mathcal{C}_2$, the boundary of an adjoining domain. With the aid of the known two-dimensional Green's function for a homogeneous space, we are then able to translate the "scattering operator" for domain $\mathcal{D}_1$ into a "reflection operator" for domain $\mathcal{D}_2$.

- Since both domains are identical, we may now combine the scattering and reflection operators for both domains into an integral equation for equivalent currents on $\mathcal{C}_1$ and $\mathcal{C}_2$. The resulting currents would produce the correct fields inside $\mathcal{D}_1$ and $\mathcal{D}_2$ in a homogeneous environment. Since the elementary solutions are known from the analysis of a single object, the superposition principle may be invoked to evaluate the field in $\mathcal{D}_1 \cup \mathcal{D}_2$.

The same procedure may be repeated to combine multiple domains. It should be remarked that subdomains need not be identical, and that the order of their combination may be chosen for convenience. Thus, we are able to combine the known portions of a complicated geometry into a fixed environment, for which a reflection operator is determined for an empty observation domain. By combining this operator with the scattering operator for an object in an empty environment, we obtain the full electromagnetic response. This enables us to optimize an object in the observation domain without re-evaluating the response of the complicated environment.

As an illustration, Figure 4 shows the field in an optimized power splitter in a finite EBG structure of 17×17 cells. In the optimization step, only the radius of a cavity at the junction between the wave-guiding channels was varied. More details can be found in [15].

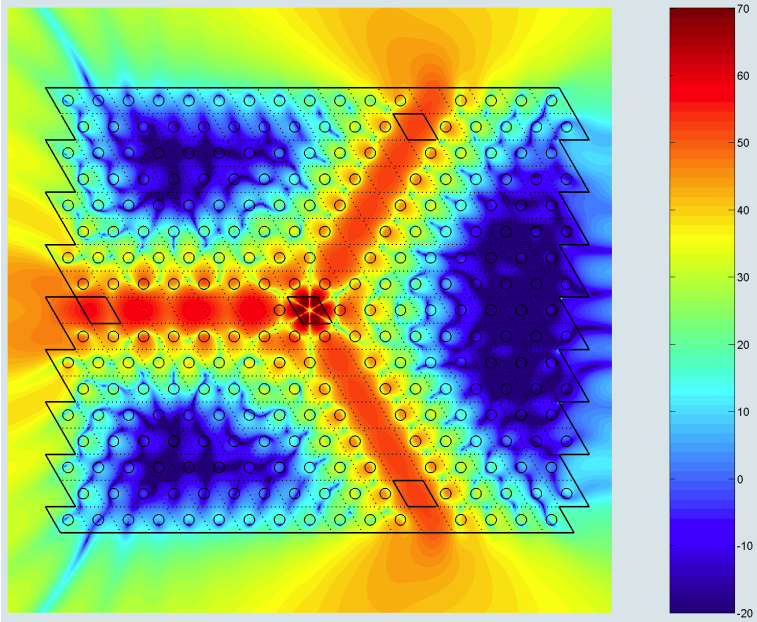

Figure 4. Electric field in an optimized power splitter (dB scale). The observation domain consisted of the four rhombic subdomains surrounded by solid lines; the remainder of the configuration was treated as the environment.

5. Deterministic Optimization

Like the forward problem, the optimization approach with which it is combined poses several challenges. We focus on two important aspects.

5.1. Choice of Cost Function

Perhaps the most difficult step in the entire procedure is the formulation of the cost function. This is where human intelligence will remain needed. This was already observed from the example of the intravascular antenna discussed in Section 3. To obtain a better impression of the difficulties that could be encountered, we chose a test structure for which reference data and engineering estimates are available from the literature [16]. We consider an infinite array of rectangular conducting patches on top of a layered dielectric slab and a ground plane, as it is presently being considered for the next generation of phased-array radar systems. To keep the analysis tractable, we approximate the feed by a vertical dipole located below the patch. An impression of a single elementary cell and the relevant physical parameters is given in Figure 5. Because of the point-source feed, we cannot determine an impedance. Instead, we consider the possibility of generating a circularly polarized wave [17].

Figure 6 shows two objective functions for a varying horizontal position of the source. All other parameters were fixed. For this case, the value of the cost function can be plotted as a function of the source coordinates x_0 and y_0. On the left, results are shown for

$$\mathrm{ERR} = \frac{|E_\theta^2 + E_\varphi^2|^2}{||E_\theta|^2 + |E_\varphi|^2|^2}, \tag{5}$$

while on the right conditions on the phase and the argument of E_θ and E_φ were combined into a single cost function. Contrary to the discussion in Section 3, we are now searching for a minimum of the function. Only

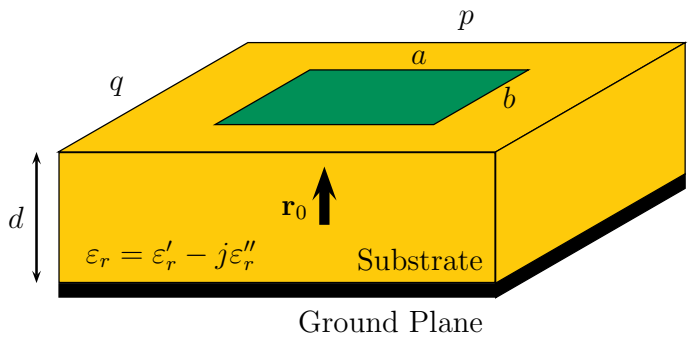

Figure 5. Element of infinite antenna array and the relevant physical parameters, i.e., $p, q, a, b, \varepsilon_r', \varepsilon_r'', d$ and the three coordinates in $\mathbf{r}_0$.

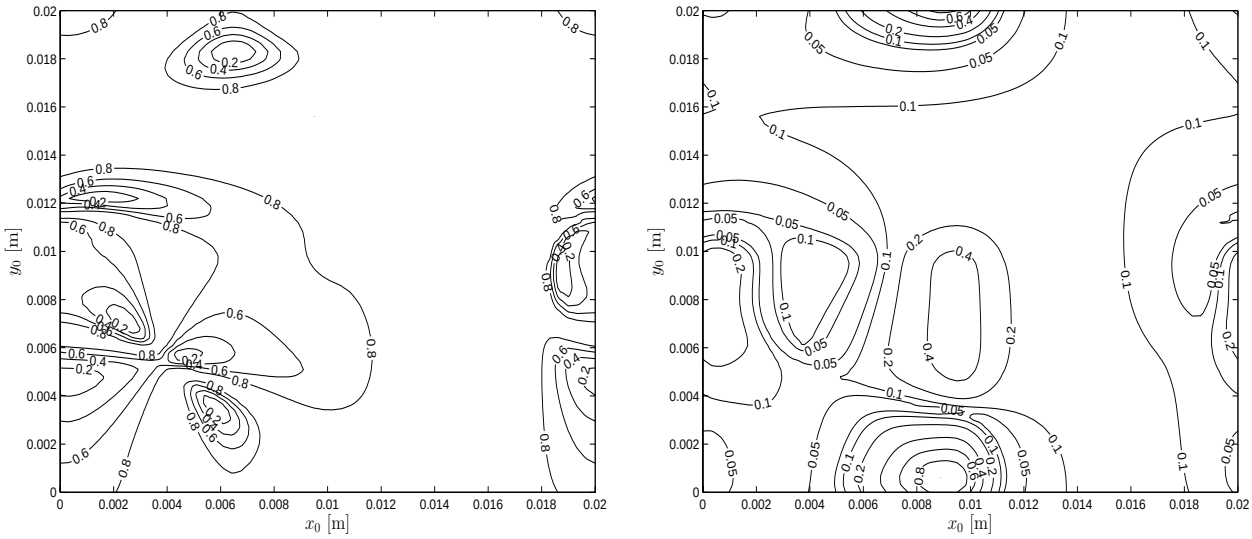

Figure 6. Objective functions for varying horizontal source coordinates x_0 and y_0. The conducting plate is located in the lower right quarter of both figures.

for the cost function in (5) convergence was obtained, with the BFGS method. The function defined in (5) equally favors left and right circular polarization. Functions for a single polarization were also investigated, and show less minima.

5.2. Sensitivity Analysis

In order to evaluate the sensitivity of the objective function with respect to a physical parameter p, we need the derivative $u'(p) = \partial_p u(p)$. In the context of a parameter sweep, it is tempting to evaluate this derivative by a finite-difference approximation of the form

$$\partial_p u_p\Big|_{p=p_m} = \frac{u(p_{m+1}) - u(p_{m-1})}{2\Delta p}. \tag{6}$$

However, when the $\{u(p_m)\}$ are evaluated by an iterative procedure, they may contain uncorrelated errors, which are enlarged by the division by the step Δp in (6). Subtracting $u(p_{m-1})$ from $u(p_{m+1})$ in the

numerator of (6) cancels the leading term in the computed results, so that the error in $u'(p)$ may become unnecessarily large.

For a single physical parameter p, differentiating (1) yields

$$L(p)\,u'(p) = f'(p) - L'(p)\,u(p), \tag{7}$$

where the prime indicates a derivative, and where $L'(p)$ and $f'(p)$ are available in closed form. By determining $u'(p)$ from (7), it is obtained with a similar accuracy as $u(p)$. The evaluation of the additional forcing term $L'(p)\,u(p)$ is usually much faster than the solution of the linear system; moreover, (1) and (7) share the same system matrix.

As an example, we show in Figure 7 results of changing the longitudinal dimension of an infinitely thin, perfectly electrically conducting rectangular plate. The conducting surface is located at $0 < x < a+\tau$, $0 < y < b$ and $z = 0$ in a Cartesian coordinate system. The plate is located in free space, and is excited by a plane wave incident from the direction $\theta = 45^\circ$, $\varphi = 90^\circ$, with the electric field polarized in the x-direction. In the space discretization of the electric-field integral equation, the domain of the plate was subdivided into elementary rectangles with dimensions $\Delta x = a/M$ and $\Delta y = b/N$, while the surface current was approximated by conventional rooftop functions. In the case of Figure 7, the dimensions of the plate are $\lambda \times \lambda$, where λ is the wavelength, and we chose $M = N = 30$. Figure 7(a) shows the result of computing $\partial_\tau J_x(x,y)|_{\tau=0}$ by analytically differentiating the electric-field integral equation as outlined in (7). The result in Figure 7(b) was obtained from the finite-difference approximation

$$\partial_\tau J_x(x,y)|_{\tau=0} = \frac{J_x(x,y)|_{\tau=\Delta\tau} - J_x(x,y)|_{\tau=-\Delta\tau}}{2\Delta\tau}. \tag{8}$$

The distributions $J_x(x,y)|_{\tau=\pm\Delta\tau}$ were obtained by adding a single row of cells to the mesh and computing the surface current density for a plate with length $a + \Delta x$, which corresponds to $\Delta x = 2\Delta\tau$. More details can be found in [18].

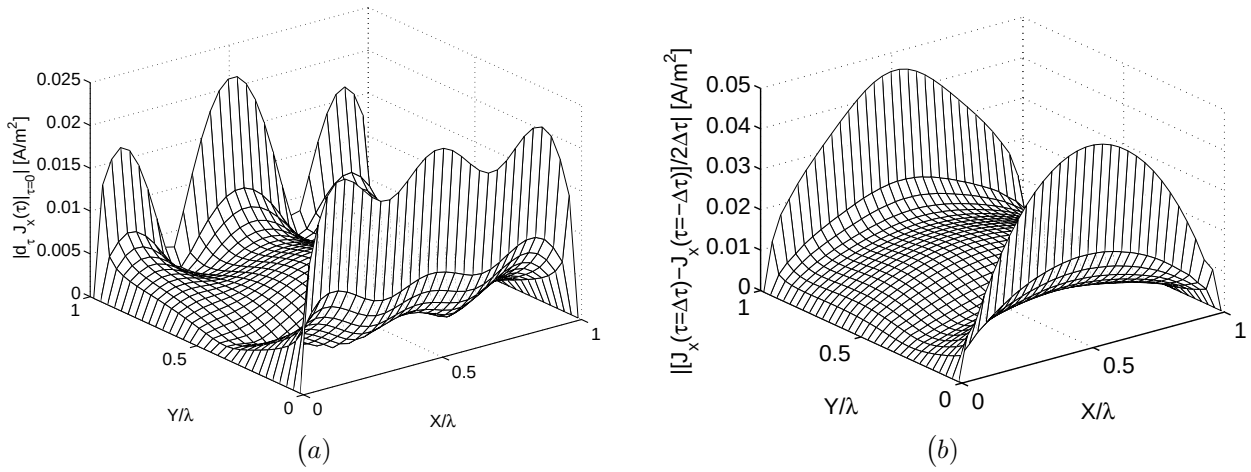

Figure 7. $\partial_\tau J_x(x,y)|_{\tau=0}$ in modulus for a $\lambda \times \lambda$ flat plate with an x-polarized plane wave incident from the direction $\theta = 45^\circ$, $\varphi = 90^\circ$. (a) shows analytic formulation and (b) shows finite-difference approximation.

It is observed that the computed results for the derivative do not match the results for the analytic formulation. The form of the distributions is different and the finite-difference result is approximately a factor

of two higher. From Figure 7 as such, it is not clear which result is correct. Therefore, we have repeated the finite-difference computation with a uniform coordinate stretch, i.e., a mesh with $\Delta x = (a + \tau)/N$ and a fixed N. The results obtained in this manner were in good agreement with the results from the analytic formulation. This indicates that the finite-difference approximation yields an unreliable estimate for the sensitivity, when applied to results obtained with a different number of cells. The explanation is that for a fixed number of cells, also the solution to the discretized integral equation depends analytically on the configuration parameters a and b, while for a changing number of cells discretization errors dominate the numerator in (8).

It could be argued that this case is somewhat pathological; the rooftop functions used to approximate the current distribution are not really adequate near the edge of the plate, and a $\lambda \times \lambda$ plate is at resonance. However, the simple test case proposed in Subsection 5.1 contains a similar plate, and in antenna optimization the desired configuration is typically at or close to a resonance. Furthermore, that test problem already has ten design parameters, i.e., $p, q, a, b, \varepsilon_r', \varepsilon_r'', d$ and the three coordinates in $\mathbf{r}_0$. This means that the generation of the search direction in each line-search step from either (6) or (7) takes an extra computational effort equivalent to performing ten field computations. On the other hand, we do not require $u(p)$, but an observable of the form

$$F(p) = \langle u(p) \mid g(p) \rangle, \tag{9}$$

where $g(p)$ is a known weighting function. Differentiating (9) with respect to a real-valued parameter p results in

$$F'(p) = \langle u'(p) \mid g(p) \rangle + \langle u(p) \mid g'(p) \rangle. \tag{10}$$

If we now solve the adjoint problem

$$L^\dagger(p) v(p) = g(p), \tag{11}$$

we can obtain the derivative of the observable $F(p)$ from

$$\begin{aligned} F'(p) &= \langle u'(p) \mid L^\dagger(p)\, v(p) \rangle + \langle u(p) \mid g'(p) \rangle \\ &= \langle L(p)\, u'(p) \mid v(p) \rangle + \langle u(p) \mid g'(p) \rangle \\ &= \langle f'(p) - L'(p)\, u(p) \mid v(p) \rangle + \langle u(p) \mid g'(p) \rangle. \end{aligned} \tag{12}$$

Thus, the evaluation of all sensitivities or Fréchet derivatives requires only one additional solution of a system of linear equations. During the line search, a single search parameter is varied, and using either (6) or (7) may be more efficient.

6. Conclusions

In this paper, we have indicated how computational electromagnetics can be used in combination with optimization algorithms to solve synthesis problems involving electromagnetic-field computations. We have proposed a two-stage procedure. In the first stage, stochastic algorithms must be employed to deal with the unavoidable occurrence of a multitude of local optima. In view of the number of field computations required, it would be best to use highly efficient approximate models involving analytical design formulas for this purpose. When an initial design is available, either from this procedure or from engineering experience, we

can proceed to the second stage, where full-wave modeling is combined with a more efficient line-search based optimization strategy. Two ideas have been proposed to reduce the computation time for a single candidate configuration: speeding up a parameter sweep by combining iterative techniques with a special extrapolation procedure, and using diakoptics to limit the computations to the part of the configuration that is subject to changes. With the aid of illustrative examples, we have demonstrated that the choice of the objective (fitness or cost) function may well be the most challenging element of the entire synthesis procedure. Finally, we have considered the Fréchet derivative. We have argued that the often employed finite-difference formula may be both unreliable and inefficient, and have proposed an alternative procedure based on analytically differentiating the underlying integral equation and solving the adjoint problem. In all cases, we have given proof of concept of our ideas with the aid of representative examples. The stochastic analysis mentioned towards the end of Section 2 was omitted from the discussion but is already being investigated in our team.

Acknowledgments

The authors gratefully acknowledge the contributions of M.J.H. Aben, R. Dirks, N.A.A. Op den Kamp and A.M. van de Water: results discussed in this paper were derived from their M.Sc. and Ph.D. Thesis research.

References

[1] L. Knockaert, D. de Zutter, "Laguerre-SVD reduced-order modelling", IEEE Trans. Microwave Theory Tech., vol. 48, pp. 2321–2329, 2004.

[2] P.J. Heres, Robust and Efficient Krylov Subspace Methods for Model Order Reduction, Ph.D. Thesis, Eindhoven, 2005.

[3] M. Webster, L. Raddatz, I. H. White, and D. G. Cunningham, "A statistical analysis of conditioned launch for gigabit ethernet links using multimode fiber", J. Lightwave Technol., vol. 17, pp. 1532–1541, 1999.

[4] William H. Press, Brian P. Flannery, Saul A. Teukolky, William T. Vetterling, Numerical Recipes, The Art of Scientific Computing, Cambridge University Press, 1988.

[5] J.M. Johnson, Y. Rahmat-Samii, Genetic Algorithms in Engineering Electromagnetics, IEEE Antennas and Propagation Magazine, Vol. 39, No. 4, pp. 7-11, August 1997.

[6] Y. Rahmatt-Samii, E. Michielsen, Electromagnetic Optimization by Genetic Algorithms, John Wiley & Sons, New York, 1999.

[7] R. Eberhart, J. Kennedy, "A new optimizer using particle swarm theory", Micro Machine and Human Science, 1995. MHS '95., Proceedings of the Sixth International Symposium on, pp. 39–43, 4–6 Oct 1995.

[8] J. Kennedy, R. Eberhart, "Particle swarm optimization", IEEE International Conference on Neural Networks, 1995. Proceedings, vol. 4, pp. 1942–1948, vol.4, Nov/Dec 1995.

[9] A.G. Tijhuis, M.C. van Beurden, A.P.M. Zwamborn, "Iterative solution of field problems with a varying physical parameter", Elektrik, vol. 10, pp. 163–183, 2002.

[10] L. Matekovits, V.A. Laza, G. Vecchi, "Analysis of large complex structures with the synthetic-functions approach", IEEE Trans. Antennas Propagat., vol. 55, pp. 2509–2521, 2007.

[11] V. Prakash, R. Mittra, "Characteristic basis function method: A new technique for efficent solution of method of moments matrix equations", Micr. Opt. Technol. Lett., vol. 36, pp. 95–100, 2003.

[12] D.J. Bekers, S.J.L. van Eijndhoven, A.A.F. van de Ven, P.-P. Borsboom, A.G. Tijhuis, "Eigencurrent analysis of resonant behavior in finite antenna arrays", IEEE Trans. Microwave Theory Tech., vol. 54, pp. 2821–2829, 2006.

[13] S. Monni, G. Gerini, A. Neto, A.G. Tijhuis, "Multimode equivalent networks for the design and analysis of frequency selective surfaces", IEEE Trans. Antennas Propagat., vol. 55, pp. 2824–2835, 2007.

[14] A.M. van de Water, B.P. de Hon, M.C. van Beurden, A.G. Tijhuis, P. de Maagt, "Linear embedding via Green's operators: A modeling technique for finite electromagnetic bandgap structures", Phys. Rev. E., vol. 72, p. 056704, 2005.

[15] A.M. van de Water, LEGO: Linear Embedding via Green's Operators, Ph.D. Thesis, Eindhoven, 2007.

[16] J.M. Jin, J.L. Volakis, "Electromagnetic scattering by a perfectly conducting patch array on a dielectric slab", IEEE Trans. Antennas Propagat., vol. 38, pp. 556–563, 1990.

[17] R. Dirks, Analysis and Optimization of Large Patch-Antenna Arrays, M.Sc. Thesis, Eindhoven, 2005.

[18] M.C. van Beurden, Integro-differential Equations for Electromagnetic Scattering: Analysis and Computation for Objects with Electric Contrast, Ph.D. Thesis, Eindhoven, 2003.